

Transplantation of Donor–Recipient Chimeric Cells Restores Peripheral Blood Cell Populations and Increases Survival after Total Body Irradiation-Induced Injury in a Rat Experimental Model

Maria Siemionow^{1,2}✉ · Małgorzata Cyran² · Katarzyna Stawarz² · Lucile Chambily² · Krzysztof Kusza³

Abstract

Current therapies for acute radiation syndrome (ARS) involve bone marrow transplantation (BMT), leading to graft-versus-host disease (GvHD). To address this challenge, we have developed a novel donor–recipient chimeric cell (DRCC) therapy to increase survival and prevent GvHD following total body irradiation (TBI)-induced hematopoietic injury without the need for immunosuppression. In this study, 20 Lewis rats were exposed to 7 Gy TBI to induce ARS, and we assessed the efficacy of various cellular therapies following systemic intraosseous administration. Twenty Lewis rats were randomly divided into four experimental groups ($n = 5$ /group): saline control, allogeneic bone marrow transplantation (alloBMT), DRCC, and alloBMT + DRCC. DRCC were created by polyethylene glycol-mediated fusion of bone marrow cells from 24 ACI (RT1a) and 24 Lewis (RT11) rat donors. Fusion feasibility was confirmed by flow cytometry and confocal microscopy. The impact of different therapies on post-irradiation peripheral blood cell recovery was evaluated through complete blood count, while GvHD signs were monitored clinically and histopathologically. The chimeric state of DRCC was confirmed. Post-alloBMT mortality was 60%, whereas DRCC and alloBMT + DRCC therapies achieved 100% survival. DRCC therapy also led to the highest white blood cell counts and minimal GvHD changes in kidney and skin samples, in contrast to alloBMT treatment. In this study, transplantation of DRCC promoted the recovery of peripheral blood cell populations after TBI without the development of GVHD. This study introduces a novel and promising DRCC-based bridging therapy for treating ARS and extending survival without GvHD.

Keywords

Acute radiation sickness • Bone marrow transplantation • Donor recipient chimeric cells • Graft versus host disease • Rat experimental model • Total body irradiation

Received: 26 February 2024 ; Accepted: 11 April 2024

© L. Hirsztfeld Institute of Immunology and Experimental Therapy, Wrocław, Poland 2024

Abbreviations

ACC, Animal Care Committee; alloBMT, allogeneic bone marrow transplantation; ARS, Acute radiation syndrome; BM, Bone marrow; BMR, Bone marrow restoration; BMT, Bone marrow transplantation; CM, Confocal microscopy; DRCC, Donor recipient chimeric cells; FC, Flow cytometry; GvHD, Graft-versus-host disease; HLA, Human leukocyte antigen; MHC, Major histocompatibility complex; PBS, Phosphate buffered saline; PKT, Paul karl horan; PLT, Platelets; RBC, Red blood cells; RGD, Rat genome database; RPMI, Roswell park memorial institute; RRID, Research resource identifiers project; SCR, Scicrunch registry; TBI, Total body irradiation; WBC, White blood cells.

1. Introduction

The constant development of medicine and the nuclear industry, the growing frequency of natural disasters, as well as an increasing threat of terrorist attacks involving nuclear power augment the possibility of radiation accidents with many casualties who may require comprehensive treatment

(Coeytaux et al. 2015). Bone marrow (BM) containing stem cells characterized by a high mitotic rate represents one of the most sensitive structures to radiation, which may result in the development of certain features associated with acute radiation syndrome (ARS) (Heslet et al. 2012). Therefore, treatment leading to bone marrow restoration (BMR) should be promptly implemented following whole-body irradiation. One of the methods currently used for managing hematopoietic ARS is bone marrow transplantation (BMT). However, serious side effects of immunosuppression and the potential risk of graft-versus-host disease (GvHD) development are associated with BMT (Billingham 1966). Due to the limited availability of effective and safe methods for treating ARS, it is crucial to search for new therapies that can positively impact BMR and thus improve the prognosis of patients exposed to high doses of radiation. The application of ex vivo created donor–recipient chimeric cell (DRCC) may act as a bridging therapy until a human leukocyte antigens (HLA)-compatible BM donor is found. The immunomodulatory potential of chimeric cells may contribute to allogeneic BM acceptance and therefore eliminate the need for immunosuppression (Cwykiel et al. 2021b).

In previously conducted studies, we introduced a novel therapy based on ex vivo created DRCC as an alternative approach to BM-based cellular therapies, aiming to support

¹ Chair and Department of Traumatology, Orthopaedics, and Surgery of the Hand, Poznań University of Medical Sciences, Poznań, Poland

² Department of Orthopaedics, University of Illinois at Chicago, Chicago, IL, USA

³ Department of Anesthesiology, Intensive Therapy and Pain Management, Poznań University of Medical Sciences, Poznań, Poland

✉ siemiom@hotmail.com; siemiom@uic.edu

tolerance induction in vascularized composite allotransplantation (Lim et al. 2018; Moris and Cendales 2021; Siemionow et al. 2023). To assess the role of hematopoietic cells in inducing mixed chimerism and immune tolerance, Cwykiel and Siemionow (2015) conducted numerous experiments creating “chimeric animals” by administering allogeneic (rat ACI, RT1a) or semi-allogeneic (rat LBN) BM cells to Lewis strains. The results obtained showed that the *in vivo* DRCC possess protolerant properties that can significantly improve the survival of complex allogeneic tissue grafts (Cwykiel and Kwiecień 2015; Cwykiel and Siemionow 2015; Cwykiel et al. 2021a).

Based on these promising findings and the successful development of rodent DRCC, we established an experimental animal model of total body irradiation (TBI). This model allowed for a comprehensive evaluation of the effects of radiation on the reconstitution of a hematopoietic system as well as the assessment of the effectiveness of BMT and DRCC therapy in the context of ARS. Our study confirmed that the application of DRCC therapy positively enhanced the values of leukocytes, lymphocytes, and erythrocytes, thereby promoting BMR following TBI. Moreover, we showed that due to the tolerogenic properties of chimeric cells and the potential for inducing mixed chimerism *in vivo* (Hivelin et al. 2016; Cwykiel et al. 2021b), treatment with DRCC is not associated with the induction of GvHD. This study confirms the possibility of clinical application of this innovative cellular therapy as a bridge treatment for patients in the course of ARS in the future.

2. Materials and Methods

2.1. Rats and animal care

This study received approval from the Animal Care Committee (ACC Number: 19-167) of the University of Illinois at Chicago, accredited by the American Association for the Accreditation of Laboratory Animal Care. All animals received humane care in compliance with the “Principles of Laboratory Animal Care” formulated by the National Society for Medical Research and the “Guide for the Care and Use of Laboratory Animal Resources” published by the US National Institutes of Health. In this experimental study, a total of 44 male Lewis rats (RT11) (strain: LEW, Research Resource Identifiers Project (RRID): Rat Genome Database (RGD)_737932) and 48 ACI rats (RT1a) (strain: ACI, RRID: RGD_737892), 8–10 weeks of age, purchased from the Charles River Laboratories (Chicago, IL, USA), were used. The animals were housed in an accredited animal facility at the University of Illinois at Chicago, where they were handled humanely according to US Public Health Service Policy. Animals were individually caged at room temperature on a 12-h day/night cycle and provided with standard rodent food and water *ad libitum*.

2.2. TBI procedure

In total, 20 male Lewis recipient rats, aged 8–10 weeks, were irradiated with a 7 Gy nonlethal dose of TBI administered at a rate of 0.4–1.0 Gy/min. The ionizing irradiation was evenly delivered using Cs-137 radionuclide via a J.L. Shepherd Irradiator, Model 143-68, ensuring a uniform dose distribution. The irradiation procedure was performed by an experienced technologist at the University of Illinois at Chicago, USA, according to the standard procedure, which required calibration of the instrument prior to irradiation and according to the established doses approved in the protocol. Throughout the irradiation procedure, rats were housed in a specially adapted metal cylinder designed for this purpose (Figure 1). Following irradiation exposure, rats were individually placed in cages with free access to antibiotic-enriched water (trimethoprim–sulfamethoxazole, 40 mg/200 mg/5 mL, Hi-Tech Pharmacal, Amityville, NY, USA) and provided with softened rodent food. Before the application of cellular therapies, rats were anesthetized with 1.5%–2.5% isoflurane inhalation, and blood samples were collected to confirm the 7 Gy TBI-induced hematopoietic injury and development of ARS.

2.3. Experimental groups

In total, 24 male fully major histocompatibility complex (MHC) mismatched ACI rats, aged 8–10 weeks, served

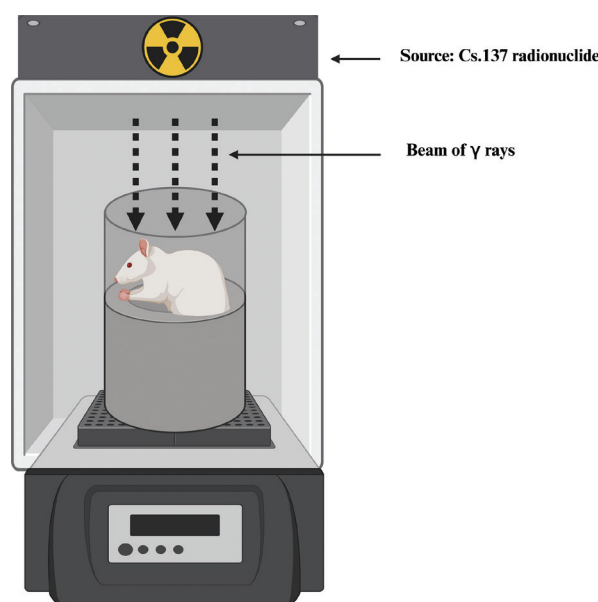


Fig 1. Experimental model of TBI for rats. Schematic image of application of the J.L. Shepherd, Model 143-68, employing Cs-137 radionuclide as the radiation source, with a metal cylinder designed for irradiation of the entire rat's body. A Lewis experimental rat is placed within a specially adapted metal cylinder designed for the procedure of whole-body irradiation. TBI, total body irradiation.

as allogeneic bone marrow transplant (alloBMT) donors. Additionally, 24 male ACI rats and 24 male Lewis rats, each aged 8–10 weeks, served as BM donors to generate DRCC. The cellular therapies were transplanted via intraosseous injection into the right femur 6 h after the irradiation procedure. Twenty Lewis rat recipients were randomly divided into four experimental groups ($n = 5/\text{group}$) and received: Group 1 control – received 0.1 mL of saline and antibiotic therapy (trimethoprim–sulfamethoxazole, 40 mg/200 mg/5 mL, Hi-Tech Pharmacal); Group 2 – was supported with alloBMT (80×10^6 cells) from the ACI donors; Group 3 – received DRCC ($4\text{--}6 \times 10^6$ cells) therapy created by the fusion of BM cells from ACI and Lewis donors; Group 4 – received alloBMT (80×10^6 cells) from the ACI donors combined with DRCC ($4\text{--}6 \times 10^6$ cells) derived from the fusion of BM cells from ACI and Lewis donors. Summary of experimental groups is presented in Table 1.

2.4. Preparation of allogeneic BM for transplantation

Twenty-four male fully MHC mismatched ACI rats, aged 8–10 weeks, were anesthetized with 1.5%–2.5% isoflurane inhalation. After induction of anesthesia, rats were euthanized with a SomnaSol solution (sodium pentobarbital 390 mg + sodium phenytoin 5 mg/mL, Henry Schein Animal Health, Melville, NY, USA) by intraperitoneal injection, with bilateral thoracotomy as an assuring method. The donors’ legs were shaved and washed with iodine solution. Both femurs and tibias were harvested under sterile conditions, then suspended in a sterile phosphate buffered saline (PBS) solution, and transferred to a sterile laminar chamber. The bones were dissected, and the intramedullary cavities were rinsed using a 3 mL syringe and an 18 G needle (305195, BD® Needle, Becton Dickinson, Franklin Lakes, NJ, USA). The bones were washed with a Dulbecco’s Modified Eagle’s Medium (DMEM, Thermo Fisher Scientific, Waltham, MA, USA) solution in the amount of 20 mL. In the next step, the cell suspension was filtered through a sterile nylon filter (pore size 40 μm) and subjected to a further purification process. Cell viability and abundance were assessed using a microscope with a Vi-CELL™ XR Cell Viability Analyzer (Beckman

Coulter, Brea, CA, USA) after the cells were stained with 0.4% Trypan Blue solution (Thermo Fisher Scientific) and plotted on a microscope slide. The isolated donor BM cells were then labeled with the fluorescent red dye Paul Karl Horan (PKH) 26GL (Sigma-Aldrich, St. Louis, MO, USA), according to the manufacturer’s instructions. The isolated and labeled ACI rat BM cells were then resuspended in 100 μL of PBS staining buffer containing 1% bovine serum albumin (BSA).

2.5. Creation of DRCC

The DRCC were created from BM cells derived from ACI and Lewis rat donors, as depicted in Figure 2a. The isolation of BM cells, creation of DRCC through the *ex vivo* cell fusion process, and evaluation of DRCC properties were thoroughly described in previous studies (Cwykiel et al. 2021a, b). Briefly, BM cells were isolated from the tibia harvested from randomly selected ACI (RT1^a) and Lewis (RT1^l) rat donors in a sterile manner and subsequently fluorescently stained using PKH26-red (ACI) or PKH67-green (Lewis) membrane dyes (Sigma-Aldrich), respectively, according to manufacturer’s instructions. Next, donor cells were mixed in a 1:1 ratio and suspended in serum-free Roswell Park Memorial Institute (RPMI) 1640 medium (Thermo Fisher Scientific). The cell fusion procedure was performed using a 1.46 g/mL polyethylene glycol (PEG) 4000 solution (EMD, Burlington, MA, USA) containing 16% DMSO (Sigma-Aldrich), as previously reported (Cwykiel and Siemionow 2014; Siemionow et al. 2015, 2018a). Fluorescence-activated cell sorting (FACS, BD FACSAria™ II cell sorter, Becton Dickinson) was applied to select the PKH26/PKH67-labeled cells, representing the DRCC population.

2.6. Flow cytometry (FC) and confocal microscopy (CM) analysis

The creation of DRCC via the *ex vivo* PEG-mediated cell fusion procedure of rat BM cells was assessed by FC and CM. Samples of unstained BM cells, the PKH26- and PKH67-stained BM cells, as well as fused PKH26/PKH67-stained DRCC were assessed using LSRFortessa™ cell cytometer

Table 1. Summary of experimental groups

Experimental group number	Type of therapy applied	Route of cells delivery	Dosage of saline/number of cells injected	Number of rats per group
Group 1	Saline	Intraosseous	0.1 mL of saline	$n = 5$
Group 2	alloBMT	Intraosseous	80×10^6 cells	$n = 5$
Group 3	DRCC	Intraosseous	$4\text{--}6 \times 10^6$ cells	$n = 5$
Group 4	alloBMT + DRCC	Intraosseous	80×10^6 cells + $4\text{--}6 \times 10^6$ cells	$n = 5$
Total number of rats ($n = 20$)				

alloBMT, allogeneic bone marrow transplantation; DRCC, donor–recipient chimeric cell.

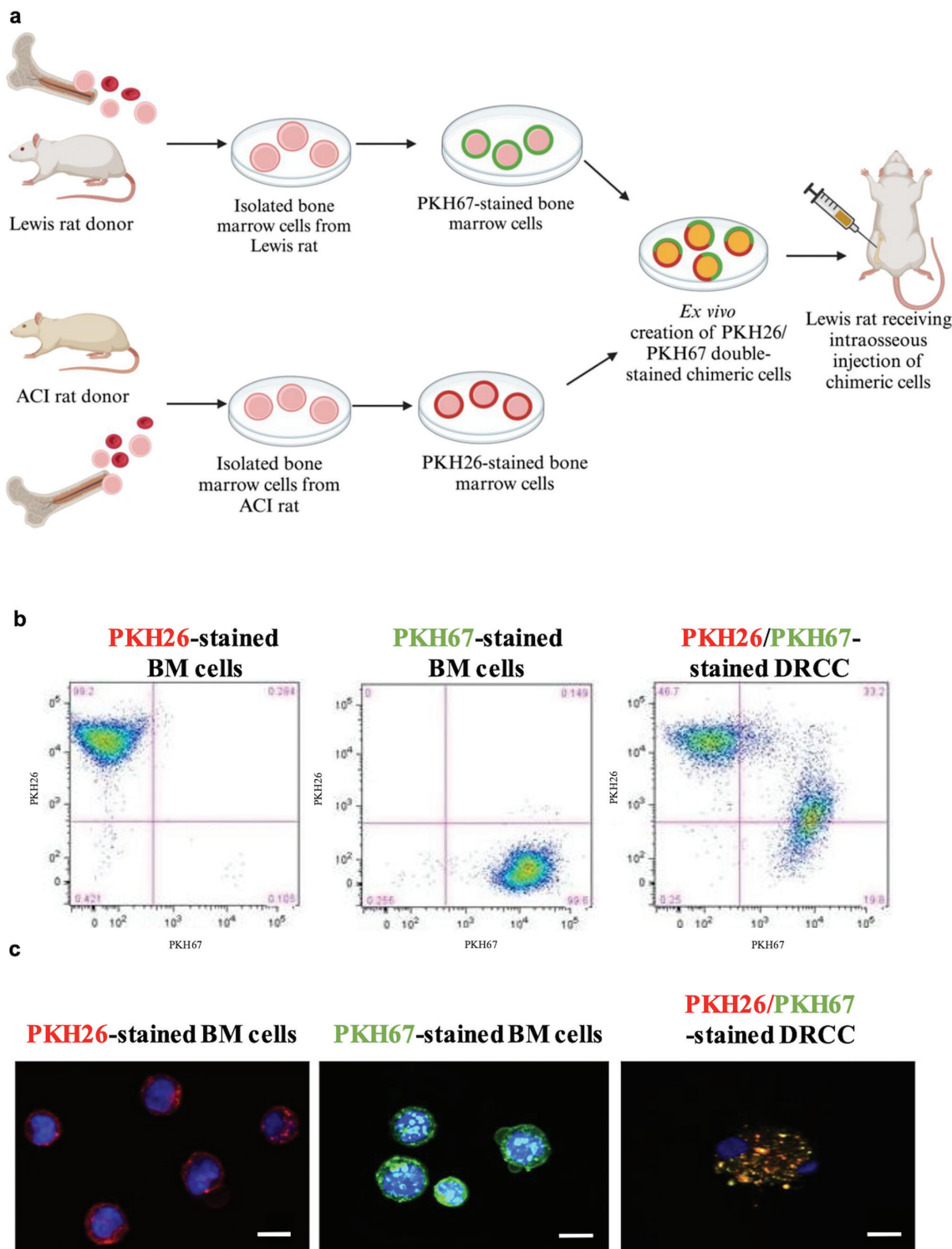


Fig 2. Confirmation of the creation of chimeric cells via *ex vivo* PEG-mediated cell fusion. (a) The study design of the creation process of DRCC from isolated BM cells of ACI and Lewis rat donors. (b) Representative FC PKH26 vs. PKH67 fluorescent labeling dot plots of (from left): PKH26-stained ACI rat BM cells; PKH67-stained Lewis rat BM cells; and fused DRCC, double-stained with PKH26/PKH67 fluorescent dyes. (c) Representative immunofluorescence CM images of (from left): PKH26-stained ACI rat BM cells (red); PKH67-stained Lewis rat BM cells (green); and fused DRCC (orange color), revealing the overlapping PKH26/PKH67 fluorescent dyes, confirming the chimeric state of the created DRCC. Images were captured using an upright confocal microscope (Leica TCS-SP2, RRID:SCR_020231), original magnification: 400 \times , scale bar: 10 μ m. BM, bone marrow; CM, confocal microscopy; DRCC, donor-recipient chimeric cell; FC, flow cytometry; PEG, polyethylene glycol.

(BD Biosciences, San Jose, CA, USA). PKH26- and PKH67-stained BM cells, and fused PKH26/PKH67-stained DRCC were fixed in 4% paraformaldehyde (EMS, Hatfield, PA, USA) and mounted with VECTASHIELD® Antifade Mounting Medium with DAPI (Vector Laboratories, Burlingame, CA, USA). Images were taken by upright confocal microscope (Leica TCS-SP2, RRID: SciCrunch Registry (SCR)_020231, Leica Microsystems, Wetzlar, Germany) with a digital camera (QImaging® Retiga-2000R Charge Coupled Device, QImaging, British Columbia, Canada) and ImagePro Plus software (RRID: SCR_016879, Media Cybernetics, Rockville, MD, USA).

2.7. Intraosseous transplantation of BM cells and DRCC

BM cells and DRCC were injected into the right femoral bone of Lewis rats, as previously reported (Siemionow et al. 2005a, b). The procedure was conducted under sterile conditions. While under general anesthesia with 1.5%–2.5% isoflurane inhalation, a 1 cm-long incision was made on the dorsal surface of the right mid-thigh of Lewis rats. Subsequently, the skin, subcutaneous tissue, and surrounding muscles were dissected, exposing the femur. Using a 0.5 mL syringe equipped with a 27 G needle (305109, BD® Needle, Becton Dickinson), a hole was created in the femoral bone, and 0.1 mL of the recipient's marrow was aspirated to prevent excessive pressure during cell injection. Then, using a 0.5 mL syringe with a 27 G needle, saline solution as control, alloBMT, or DRCC suspended in sterile saline solution, or a combination therapy comprising alloBMT and DRCC suspension was injected into the femur through a pre-made hole, depending on the belonging to the experimental group. Following the intraosseous injection, the bone opening was sealed with bone wax (Medeline Industries, Mundelein, IL, USA) to prevent cell leakage from the marrow cavity. The muscles and skin were sutured using 4–0 and 5–0 absorbable sutures (Ethicon Inc., Raritan, NJ, USA), respectively. Post-operatively, rats recovered in a heated environment and received necessary care before returning to the colony.

2.8. Survival and body weight assessment

The rats underwent daily observations to assess their survival rates over the entire 90-day observation period. The baseline body mass of each animal was recorded at the beginning of the study and was then measured daily during the initial 8 days and subsequently, every other day throughout the entire 90-day follow-up period. To address the weight differences between animals assigned to the four experimental groups at the study beginning before irradiation, adjustments were done using Microsoft Excel (ver.16.0, Reman, WA, USA) software. Therefore, the initial weight on day 0 was set as a baseline, denoted as 100%, and the subsequent weights were then

calculated as the percentage relative to this baseline value. These percentage values were calculated in 10-day intervals until the end of the 90-day observation period.

2.9. Blood sampling procedure

Peripheral blood samples (0.3 mL) were obtained from the jugular vein on day 0 as a baseline reference sample, prior to TBI and the administration of cell therapies. Subsequent samples were collected on days 5, 10, 20, 30, 40, 60, and 90 following TBI for further analysis. During the procedure, rats were anesthetized with 1.5%–2.5% isoflurane inhalation. Blood samples were collected in ethylenediaminetetraacetate collection tubes (BD Microtainer®, Becton Dickinson) and immediately processed by the accredited Biologic Resources Laboratory at the University of Illinois at Chicago, for complete blood counts, including white blood cells (WBC), WBC differentials (neutrophils, lymphocytes, monocytes, eosinophils, and basophils), red blood cells (RBC), and platelets (PLT). At the 90-day study end-point, rats were euthanized using SomnaSol solution (sodium pentobarbital 390 mg + sodium phenytoin 5 mg/mL, Henry Schein Animal Health) by intra-peritoneal injection, followed by the bilateral thoracotomy as an assuring method.

2.10. Clinical observations

After the intraosseous transplantation of BM cells and DRCC therapies, animals were observed for signs of morbidity and symptoms of GvHD, daily for the first 8 days, and subsequently, every other day over the entire follow-up period of 90 days. The animals had free access to antibiotic-enriched water (trimethoprim–sulfamethoxazole, 40 mg/200 mg/5 mL, Hi-Tech Pharmacal) and softened rodent food. A summary of the assessed clinical parameters and total scores is presented in Table 2. The analysis included implementation of scores for activity in the cage, body posture, fur coverage, presence of blood in the stool, and diarrhea incidence for each individual animal. These scores were then summarized and divided by the total number of observations. Activity in the cage, body posture, and fur coverage were assessed on a scale ranging from 0 to 3 points, where 0 = a normal response and 3 = the most pronounced abnormality. Incidences of blood in stool and diarrhea were evaluated on a scale from 0 to 1, where 0 represented the absence of blood in stool or normal stool consistency, and 1 indicated the presence of blood in stool or diarrhea. All rats underwent evaluation using two total score systems. The first score system, ranging from 0 to 9 points, assessed the overall physical condition, which included parameters such as activity in the cage, body posture, and fur coverage. The second score system, ranging from 0 to 2 points, focused on the digestive

distress conditions, considering the presence of blood in the stool and the incidence of diarrhea.

2.11. Assessment criteria for GvHD

The histological assessment of GvHD included examination of the kidney, skin, and small intestine biopsies. Tissue biopsies were collected on the 90th day and placed in a formalin solution for 48 h. Subsequently, tissue samples were fixed in a 70% ethanol solution and embedded in paraffin blocks. These paraffin blocks were then sliced into 0.5 mm thick sections using a microtome (2088 Ultratome® V Microtome, LKB Bromma, Amersham, UK) and affixed to microscope slides. The preparations included Hematoxylin and Eosin staining according to a standard protocol. The histopathological evaluation of GvHD changes was performed by the use of a BX51/IX70 inverted microscope (Olympus, Tokyo, Japan). The presence of histopathological changes in the course of GvHD was assessed in accordance with the Small Criteria presented in Table 3. The criteria assessing the degree of GvHD occurrence, based on the examined organ, are outlined in Table 4. Each tissue biopsy was assigned a numerical score on a scale from 0 to 3 points, depending on the changes suggesting the GvHD occurrence, where the value 0 = no GvHD, the value 1 = GvHD possible, the value 2 = consistent with GvHD, and the value 3 = definite GvHD (Shulman et al. 2015). The closer the score was to zero, the less likely the assessed sample exhibited signs of GvHD.

2.12. Statistical analysis

Data are expressed as the mean \pm standard error of the mean (SEM). GraphPad Prism (ver.9.2.1, RRID: SCR_002798, Dotmatics, Boston, MA, USA) software and Microsoft Excel (ver.16.0, Microsoft Corporation) were used to perform statistical analysis. Two-way analysis of variance (ANOVA) for group comparison was used to define statistical significance. Results were considered statistically significant for $p < 0.05$. The graphs represent mean values with SEM, statistical significance is marked with asterisks: * $p < 0.05$, ** $p < 0.01$, *** $p < 0.001$, **** $p < 0.0001$.

3. Results

3.1. Confirmation of DRCC creation via *ex vivo* PEG-mediated fusion

The study design of the *ex vivo* PEG-mediated cell fusion procedure of the rat BM cells derived from ACI and Lewis donors is presented in Figure 2a. The DRCC population demonstrated >95% purity and the efficacy of the donor and recipient cell fusion was assessed at 32.2%, as confirmed by FC analysis (Figure 2b). The efficacy of the fusion procedure and the quality of the created chimeric cells were further confirmed by CM, revealing the presence of overlapping PKH26/PKH67 fluorescent staining confirming the chimeric state of the created DRCC (Figure 2c). The presented data confirmed the successful creation of DRCC from ACI and Lewis BM cells by FC and CM analyses.

Table 2. Clinical parameters evaluated over 90 days post-7 Gy TBI and different cellular therapy administrations

Clinical parameters	Ratings	Score system
Activity in the cage	0- Very active animal, moving in the cage, typical gait 1- Slightly decreased degree of activity, gait mildly disturbed 2- Animal moving very slowly, gait severely disturbed 3- Animal reluctant to move or lack of any movement	0–3 points
Body posture	0- Normal body posture 1- Slightly hunched over 2- Moderately hunched over 3- Very hunched over	0–3 points
Fur coverage	0- Normal fur condition 1- No fur loss and spiky fur 2- Moderate fur loss and raised fur 3- Significant fur loss and bristling fur	0–3 points
Overall physical condition total score = 0–9 points		
Blood in stool incidence	0- Absence of blood in stool 1- Presence of blood in stool	0–1 point
Diarrhea incidence	0- Absence of diarrhea, normal stool consistency 1- Presence of diarrhea	0–1 point
Digestive distress condition total score = 0–2 points		

TBI, total body irradiation.

Table 3. Histopathological changes constituting the Small Criteria for assessing the degree of GvHD occurrence

Kidney	Skin	Small intestine
Tubulointerstitial inflammation, basement membrane nephropathy, microangiopathy, fibrinoid necrosis (segmental or global), interstitial fibrosis, tubular necrosis	Vacuolar degeneration, epidermal necrosis, lichenification, inflammation of the skin appendages, non-specific lymphocytic dermatitis, apoptosis and dermal keratosis, fibrosis of the dermis, hyperkeratosis of the epidermis, acanthosis, spongiotic dermatitis with marked spongiosis	Non-specific mucositis, gland damage, mucosal damage, the presence of crypt distortion, active inflammation, Paneth cell metaplasia, degree of mucosal fibrosis, apoptotic changes within crypts, the presence of intestinal endothelial lymphocytes

GvHD, graft-versus-host disease.

Table 4. Criteria for assessing the degree of GvHD occurrence based on histopathological changes

Degree of GvHD occurrence (score)	No GvHD (0)	GvHD possible (1)	Consistent with GvHD (2)	Definite GvHD (3)
Kidney	No deviation	Presence of <2 small criteria	Presence of ≥2 small criteria without the presence of basement membrane nephropathy	Presence of basement membrane nephropathy
Skin	Presence of one small criterion or the absence of deviations	Presence of ≥2 small criteria or the presence of apoptosis	Presence of lichenification, dermal fibrosis, spongiosis without apoptosis, or presence of apoptosis with small criteria but excluding lichenification and spongiosis	Occurrence of apoptosis with lichenification and acanthosis or spongiosis
Small intestine	Presence of one small criterion or the absence of deviations	Presence of ≥2 small criteria or small criteria without the presence of crypt apoptosis	Presence of ≥2 small criteria in the presence of 2–5 apoptotic crypts	Presence of >6 apoptotic crypts with at least one small criterion

GvHD, graft-versus-host disease.

3.2. Transplantation of alloBMT results in the highest mortality rate following 7 Gy TBI

Following 7 Gy TBI, there was a 60% mortality rate in the group receiving alloBMT therapy, whereas a 100% survival rate was observed in the other therapy groups and the control group (Figure 3). Animals that did not survive until the end of the observation period displayed a gradual decline in activity, pallor, changes in fur condition, a slumped body posture, and the presence of blood in the stool. Rat mortality occurred naturally on days 10, 11, and 12 following TBI and alloBMT administration; therefore, no euthanasia procedures were performed in these cases.

3.3. Confirmation of body weight maintenance over a 90-day observation period following 7 Gy TBI

The changes in rats' body weight over a 90-day observation period following 7 Gy TBI and administration of different cellular therapies are presented in Figure 4. There was a decrease in body weight from across all experimental groups from the beginning of the observation period until the 5th day, followed by a subsequent increase in body weight during the remaining observation period up to 90 days following irradiation exposure. Additionally, at

the 30-day observation, a decrease in body weight was observed in the DRCC therapy group, which was subsequently regained in the following weeks. In summary, aside from the initial post-irradiation drop in body weights, animals across all experimental groups regained body weight, surpassing the initial body weight values. This recovery was evidenced by body weight changes exceeding 100%. The regained weight was then maintained throughout the 90-day observation period.

3.4. Application of DRCC therapy facilitates peripheral blood cell populations recovery following 7 Gy TBI

The summary of the peripheral blood cells populations changes observed in the WBC, lymphocytes, monocytes, neutrophils, basophils, and eosinophils as well as in RBC and PLT values over the 90-day observation period following 7 Gy TBI and the administration of different cellular therapies is presented in Figure 5. The baseline values represent measurements taken before TBI and the administration of cellular therapies and served as a reference for comparative analysis.

On day 0 before TBI and application of cell therapies, assessment of WBC counts revealed higher baseline WBC values in the DRCC therapy group when compared to the

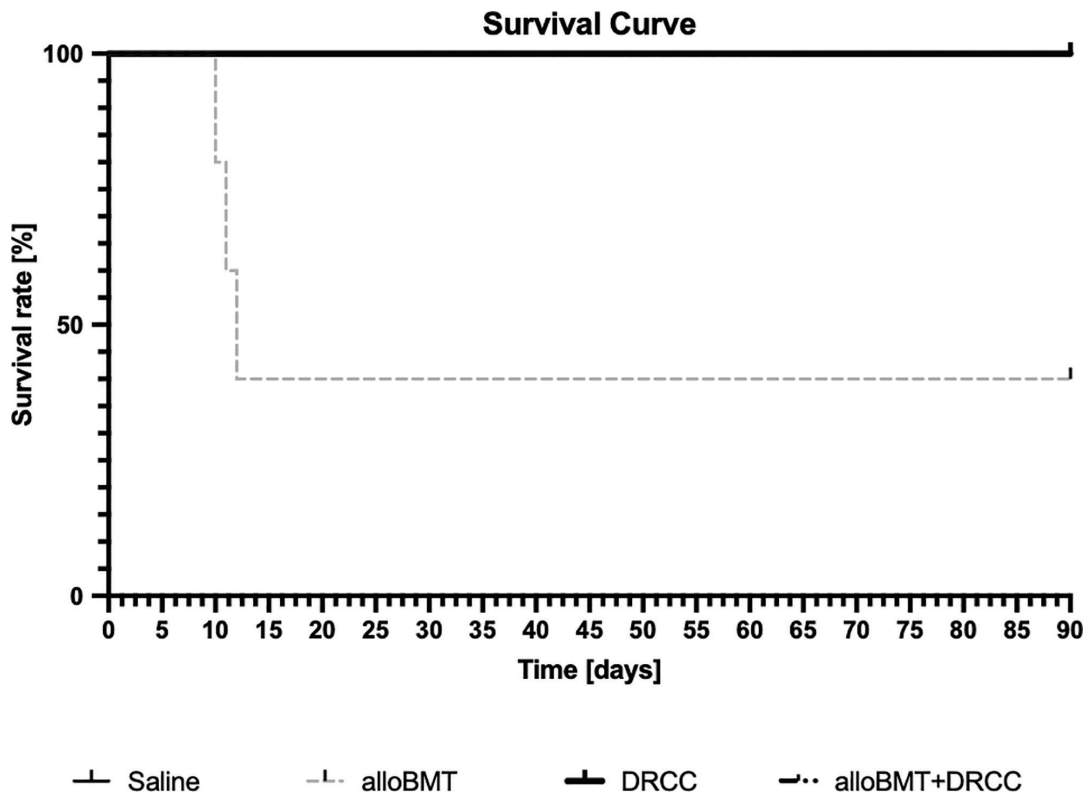


Fig 3. Survival rate changes post-7 Gy TBI with different cellular therapies over a 90-day observation. The highest mortality rate of 60% was observed following administration of the alloBMT therapy. In contrast, 100% survival rate was observed in all the remaining experimental groups. alloBMT, allogeneic bone marrow transplantation; DRCC, donor recipient chimeric cells; TBI, total body irradiation.

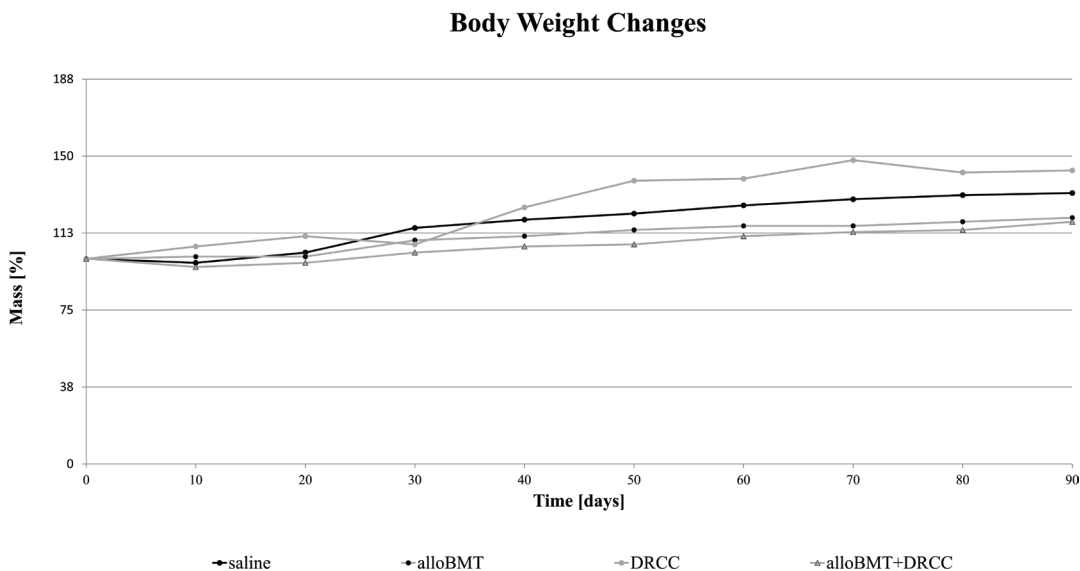


Fig 4. Body weight changes post-7 Gy TBI with different cellular therapies during a 90-day observation. There were differences in the initial body mass between the animals assigned to the four experimental groups. The initial weight on day 0 was set as a baseline, denoted as 100%, and the subsequent weights were then calculated as the percentage relative to this baseline value. These percentage values were calculated in 10-day intervals until the end of the 90-day observation period. Ultimately, rats in all experimental groups regained their body weight, surpassing the initial values by the end of the observation period. alloBMT, allogeneic bone marrow transplantation; DRCC, donor recipient chimeric cells; TBI, total body irradiation.

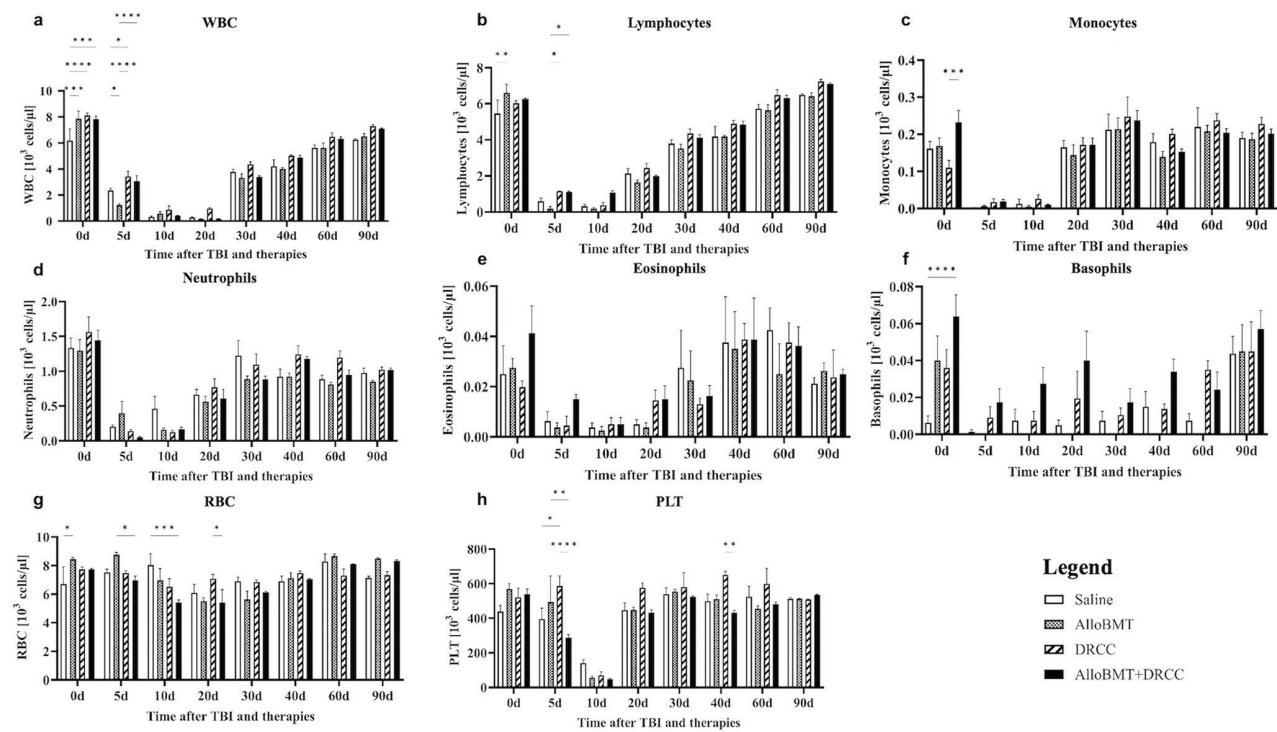


Fig 5. Cellular therapy's impact on peripheral blood cell populations during 90-day observation post 7 Gy TBI. Assessment of the peripheral blood cells population counts after application of alloBMT, DRCC, and alloBMT + DRCC therapies following 7 Gy TBI confirmed the restoration of hematopoietic cells by DRCC therapy. The highest (a) WBC values were observed in the DRCC and alloBMT + DRCC groups throughout the entire 90 days follow-up. Also, the highest (b) lymphocyte values were observed in the DRCC and alloBMT + DRCC groups over the entire observation period. The only significant difference was observed in the (c) baseline monocyte values between the alloBMT + DRCC group and the DRCC therapy. No statistically significant differences were found in the values of (d) neutrophils or (e) eosinophils between all the experimental groups. The only difference in (f) basophil counts was observed in the baseline values of the alloBMT + DRCC and control groups. (g) RBC counts were comparable among the tested therapies, following a similar trend during the 90-day observation period. After the initial drop, (h) PLT counts exhibited an increase, with the highest values observed in the DRCC therapy group over the entire follow-up period. Data presented as mean \pm SEM. One-way ANOVA test * $p < 0.05$, ** $p < 0.01$, *** $p < 0.001$, **** $p < 0.0001$. alloBMT, allogeneic bone marrow transplantation; ANOVA, analysis of variance; DRCC, donor–recipient chimeric cell; PLT, platelets; RBC, red blood cells; SEM, standard error of the mean; TBI, total body irradiation; WBC, white blood cells.

control group (8.116 ± 0.179 vs. 6.190 ± 0.888 , respectively, $p < 0.0001$). Similarly, higher WBC counts were observed in the alloBMT group compared to the control group (7.864 ± 0.582 vs. 6.190 ± 0.888 , respectively; $p < 0.001$). Moreover, higher WBC counts were also seen in the alloBMT + DRCC therapy group when compared to the control group (7.383 ± 0.229 vs. 6.190 ± 0.888 , respectively; $p < 0.001$).

On day 5 after TBI and application of cell therapies, the DRCC therapy group exhibited almost a three-fold increase in WBC counts compared to the alloBMT group (3.428 ± 0.402 vs. 1.238 ± 0.110 , respectively; $p < 0.0001$). In addition, increased WBC counts were observed in the DRCC group compared to the control group (3.428 ± 0.402 vs. 2.363 ± 0.146 ; respectively, $p < 0.05$). Furthermore, a three-fold increase in WBC counts was observed in alloBMT + DRCC compared to alloBMT therapy (3.073 ± 0.421 vs. 1.238 ± 0.110 , respectively; $p < 0.0001$). Finally, the WBC counts recorded in the control group were almost twice as high as those in the

alloBMT therapy group (2.363 ± 0.146 vs. 1.238 ± 0.110 , respectively; $p < 0.05$) (Figure 5a).

On day 0 before TBI and application of cell therapies, lymphocyte baseline values in the alloBMT group were significantly higher compared to the control group (6.609 ± 0.467 vs. 5.460 ± 0.746 , respectively; $p < 0.01$) (Figure 5b).

On day 5 after TBI and application of cell therapies, lymphocyte counts showed a six-fold increase following administration of DRCC therapy when compared to the alloBMT (1.148 ± 0.031 vs. 0.185 ± 0.12 ; respectively, $p < 0.05$). Similarly, the lymphocyte counts in the alloBMT + DRCC therapy group exhibited a six-fold increase compared to the alloBMT group (1.108 ± 0.047 vs. 0.185 ± 0.121 , respectively; $p < 0.05$).

On day 0 before TBI and application of cell therapies, the only notable increase in monocyte counts was observed in the alloBMT + DRCC group when compared to the DRCC therapy group, relative to the baseline values (0.169 ± 0.021 vs. 0.110 ± 0.019 , respectively; $p < 0.0001$) (Figure 5c).

No significant differences were observed in neutrophil or eosinophil counts among the administered cellular therapies (Figures 5d and 5e).

On day 0 before TBI and application of cell therapies, the assessment of baseline basophil counts revealed significantly higher values in the alloBMT + DRCC group when compared to the control group (0.064 ± 0.012 vs. 0.006 ± 0.004 , respectively; $p < 0.0001$) (Figure 5f). Following TBI, the monocyte counts revealed initial decline between days 5 and 10, followed by a gradual increase from day 20 onward throughout the remaining observation period, reaching the highest values in the DRCC therapy group on days 30, 40, 60, and 90.

On day 0 before TBI and application of cell therapies, the mean baseline RBC values in the alloBMT therapy group were higher compared to the control group (8.449 ± 0.120 vs. 6.709 ± 1.200 , respectively; $p < 0.05$) (Figure 5g).

On day 5 after TBI and application of cell therapies, the RBC values were higher in the alloBMT compared to the alloBMT + DRCC therapy group (8.770 ± 0.146 vs. 6.973 ± 0.291 , respectively; $p < 0.05$).

On day 10 after TBI and application of cell therapies, there was a 1.5-fold increase in RBC values recorded in the control group compared to the alloBMT + DRCC group (8.038 ± 0.808 vs. 5.423 ± 0.175 , respectively; $p < 0.001$).

On day 20 after TBI and application of cell therapies, a 1.3-fold increase in RBC values was observed in the DRCC group compared to the alloBMT + DRCC group (7.086 ± 0.302 vs. 5.400 ± 0.920 , respectively; $p < 0.05$) (Figure 5g).

On day 5 after TBI and application of cell therapies, PLT counts analysis revealed two-fold increase in the DRCC therapy group compared to the alloBMT + DRCC group (586.0 ± 59.093 vs. 287.75 ± 18.759 , respectively; $p < 0.0001$). Also, PLT counts were significantly higher in the DRCC group compared to the control group (586.0 ± 59.093 vs. 395.50 ± 62.8 , respectively; $p < 0.05$) and in the alloBMT group, compared to the alloBMT + DRCC therapy group (494.0 ± 149.346 vs. 287.7 ± 18.75 , respectively; $p < 0.01$) (Figure 5h).

On day 40 after TBI and application of cell therapies, a 1.4-fold increase in the PLT values was recorded in the DRCC therapy group when compared to the alloBMT + DRCC group (650.5 ± 21.683 vs. 432.5 ± 12.906 , respectively; $p < 0.01$) (Figure 5h).

3.5. Combined alloBMT and DRCC therapy decreases the severity of clinical symptoms of GvHD

A summary of the assessed clinical parameters is presented in Table 2. The analysis included the assessment of scores for the animals' activity in the cage, the presence of blood in the stool, the body posture, incidence of diarrhea, and the fur coverage for each individual animal, and the scores were summarized and divided by the total number of observations (Table 5). Activity in the cage, the body posture, and fur coverage were assessed on

a scale ranging from 0 to 3 points, where 0 = a normal response and 3 = the most pronounced abnormality. Presence of blood in the stool and the incidence of diarrhea were evaluated on a scale from 0 to 1, where 0 = the absence of blood in stool or normal stool consistency, and 1 = the presence of blood in stool or diarrhea. The closer the score was to zero, the more closely the assessed feature aligned with the normal clinical conditions. Subsequently, all rats were evaluated using two total score systems. The first score system, ranging from 0 to 9 points, assessed the overall physical condition, which included parameters such as activity in the cage, body posture, and fur coverage. The second score system, ranging from 0 to 2 points, focused on digestive distress conditions, considering the presence of blood in the stool and incidence of diarrhea. The poorest activity was recorded in the control saline group (0.96 ± 0.453) and the alloBMT + DRCC therapy group (0.29 ± 0.302) (Table 5). The activity closest to normal was observed in the alloBMT group (0.13 ± 0.031). The difference between the alloBMT and the control group was statistically significant (0.13 ± 0.031 vs. 0.96 ± 0.453 , respectively; $p < 0.05$). The body posture exhibiting minimal changes was observed in the alloBMT + DRCC (0.00 ± 0.000) and DRCC therapy (0.02 ± 0.027) groups, whereas the most significant changes in body posture were seen in animals receiving alloBMT (0.34 ± 0.227). The differences between the alloBMT and the alloBMT + DRCC therapy group were statistically significant (0.34 ± 0.227 vs. 0.00 ± 0.000 , respectively; $p < 0.05$). Assessment of fur coverage in the DRCC therapy group revealed scores close to normal fur coverage (0.51 ± 0.118). Similar trend in fur coverage was observed in animals receiving alloBMT + DRCC therapy (0.60 ± 0.094). In contrast, animals supported with the alloBMT showed the most advanced changes in fur coverage (1.15 ± 0.273). There was a significant difference in the fur coverage score in the DRCC compared to the alloBMT group (0.51 ± 0.118 vs. 1.15 ± 0.27 , respectively; $p < 0.05$). The presence of blood in the stool was notably more frequent in rats receiving alloBMT compared to the alloBMT + DRCC therapy (0.19 ± 0.194 vs. 0.07 ± 0.023 , respectively; $p < 0.05$). The most frequent occurrence of diarrhea was observed in the control (0.16 ± 0.118) and the alloBMT + DRCC therapy (0.08 ± 0.027) groups, and least frequently among animals receiving DRCC therapy (0 ± 0.009). There were significant differences in the frequency of diarrhea occurrence between the control and DRCC therapy group (0.16 ± 0.118 vs. 0 ± 0.009 , respectively; $p < 0.05$). Overall, the clinical changes closest to normal were observed in the DRCC therapy group, with an overall physical condition total score of 0.78 and a digestive distress condition total score of 0.06. In the remaining experimental groups, mild changes were observed, with the most pronounced changes noted in the control group, which exhibited an overall physical condition total score of 1.68 and a digestive distress condition total score of 0.34. Following closely, the alloBMT group displayed total scores of 1.62 and 0.28 for overall physical condition and digestive condition,

Table 5. Comparison of clinical parameters after 7 Gy TBI and different cellular therapy administration

Experimental groups	Activity in the cage (0–3)	Body posture (0–3)	Fur coverage (0–3)	Overall physical condition total score (0–9)	Blood in stool (0–1)	Diarrhea incidence (0–1)	Digestive distress condition total score (0–2)
Saline control	0.96 ± 0.453*	0.02 ± 0.026	0.70 ± 0.089	1.68	0.18 ± 0.187	0.16 ± 0.118*	0.34
alloBMT	0.13 ± 0.031*	0.34 ± 0.227*	1.15 ± 0.273*	1.62	0.19 ± 0.194*	0.09 ± 0.025	0.28
DRCC	0.25 ± 0.303	0.02 ± 0.027	0.51 ± 0.118*	0.78	0.06 ± 0.025	0.00 ± 0.009*	0.06
alloBMT + DRCC	0.29 ± 0.302	0.00 ± 0.000*	0.60 ± 0.094	0.89	0.07 ± 0.023*	0.08 ± 0.027	0.15

Data presented as mean ± SEM. One-way ANOVA test **p* < 0.05.
alloBMT, allogeneic bone marrow transplantation; ANOVA, analysis of variance; DRCC, donor recipient chimeric cells; SEM, standard error of the mean; TBI, total body irradiation.

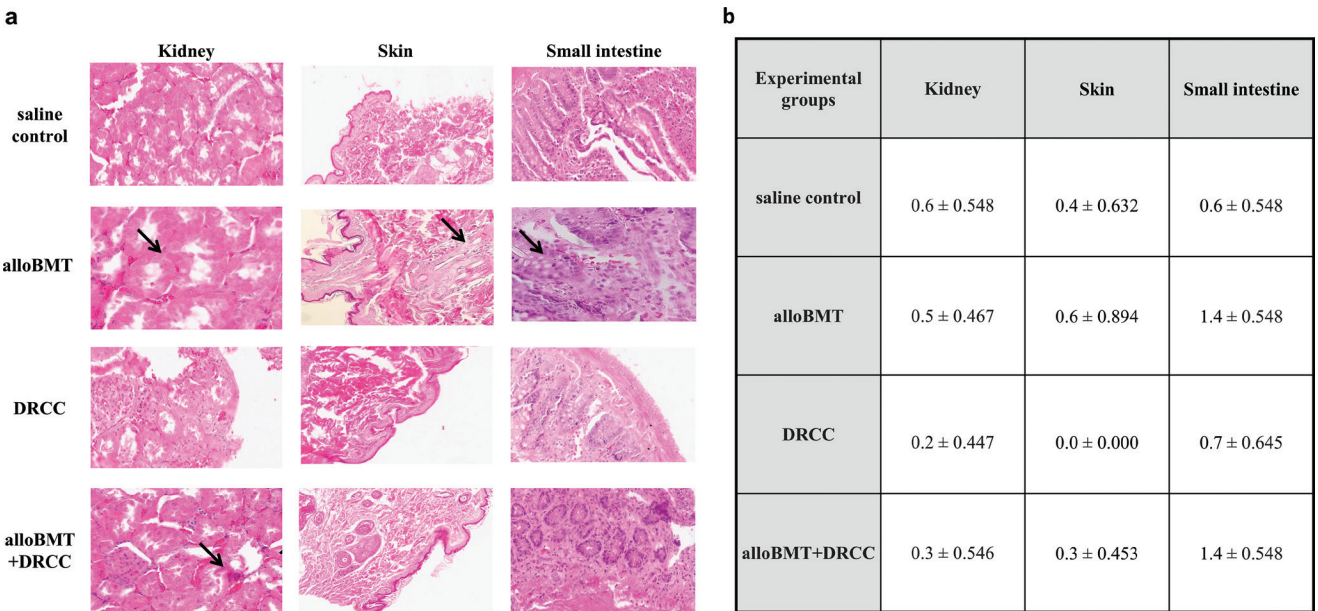


Fig 6. Cellular therapy's effect on kidney, skin, and small intestine histopathology 90 days post-7 Gy TBI. (a) Representative images of Hematoxylin and Eosin stained cross-sections of kidney, skin, and small intestine of Lewis rats at 90 days following 7 Gy TBI and application of: saline control, alloBMT, DRCC, and alloBMT + DRCC therapies. In renal tissue images, inflammatory changes and necrosis within the tubules were observed following alloBMT and alloBMT + DRCC therapies, respectively, as indicated by the arrow. Following DRCC therapy, no inflammation was observed within the examined tissues. Skin tissue images showed inflammatory infiltration of the appendages after alloBMT therapy, as demonstrated by the arrow. In the small intestine tissue sample, an apoptotic body marked by the arrow was observed following alloBMT therapy. Magnification: 20 × . (b) The lowest incidence of GvHD on the renal tissue samples was observed in the DRCC group, compared to the highest incidence seen in the saline control group. Based on the assessment of the skin tissue samples, the highest score suggesting GvHD was recorded in the alloBMT group, whereas the lowest score was found in the DRCC group. Furthermore, the highest score of GvHD on slides of the small intestine samples was assessed in both the alloBMT and alloBMT + DRCC groups, while the lowest score was observed in the control group. Data presented as mean ± SEM. alloBMT, allogeneic bone marrow transplantation; DRCC, donor recipient chimeric cells; GvHD, graft-versus-host disease; SEM, standard error of the mean; TBI, total body irradiation.

respectively. In comparison, the alloBMT + DRCC group demonstrated lower total scores, with values of 0.89 for overall physical condition and 0.15 for digestive distress condition.

3.6. DRCC therapy reduces symptoms of GvHD following 7 Gy TBI

Comparisons of histopathological changes assessed in the tissue biopsies collected from kidney, skin, and small intestine

suggesting presence of GvHD are presented in Figure 6a. For histological assessment, each tissue sample was assigned a numerical score on a scale from 0 to 3 points, depending on the changes suggesting the occurrence of GvHD, where score 0 = no GvHD, score 1 = GvHD possible, score 2 = consistent with GvHD, and score 3 = definite GvHD (Shulman et al. 2015). The closer the score was to zero, the less likely the assessed sample exhibited signs of GvHD. The criteria assessing the degree of the GvHD occurrence, based on the examined organ,

are outlined in Table 4. The lowest score suggesting the occurrence of GvHD on kidney tissue histological slides was noted in animals receiving DRCC therapy (0.2 ± 0.447), while the highest score was found in the control group (0.6 ± 0.548) (Figure 6b). Based on the histological assessment of skin slides, the highest score for GvHD occurrence was found in animals receiving alloBMT (0.6 ± 0.894), and the lowest score was found in the DRCC therapy group (0.0 ± 0.000). Additionally, the highest score indicating the possible presence of GvHD on the histological slides of small intestine tissue was observed in animals subjected to alloBMT (1.4 ± 0.548) and alloBMT + DRCC therapy (1.4 ± 0.548), whereas the lowest score was found in the control group (0.6 ± 0.548). A similar score indicating GvHD occurrence in small intestine slides was observed in the DRCC therapy group (0.7 ± 0.645). Overall, no significant histological changes indicative of GvHD were observed in the tissue samples of the kidney, skin, and small intestine in the DRCC group. In contrast, changes indicative of GvHD were present in all three tissue biopsies in the alloBMT group, including the skin. Although the scores in kidney and small intestine samples were higher in the alloBMT group when compared to the DRCC group, the differences were not significant, but the DRCC therapy reduced signs indicative of GvHD.

4. Discussion

In the last decade, we witnessed an increased risk of terrorist attacks using different types of weapons and a steady increase in the use of nuclear energy in many industries, which implicates the potential risk of nuclear disaster and the development of the ARS in the affected population (Hagby et al. 2009). Depending on the absorbed irradiation dose, various ARS signs may occur. Initial signs and symptoms encompass nausea, vomiting, diarrhea, hematochezia, inflammation, fatigue, and fever (Mettler et al. 2007). Nevertheless, ARS may progress to disseminated coagulopathies, sepsis, or acute respiratory failure, culminating in irradiation-induced multi-organ failure with a poor prognosis (Mettler et al. 2007). Despite numerous studies on methods of treating ARS, the treatment options used so far remain unsatisfactory. Current approaches primarily include alloBMT therapy, which carries the risk of GvHD. Moreover, alloBMT requires the use of immunosuppression protocols, which carry significant side effects (Basic-Jukić and Labar 2003). Furthermore, ethical considerations preclude research on new treatment methods for ARS in humans, and the available data are primarily derived from the analysis of victims of radiation accidents (Baranov et al. 1989; Basic-Jukić and Labar 2003; Hiramata et al. 2003; Mettler et al. 2007; Gourmelon et al. 2010; Ostheim et al. 2021). Hence, there is urgent need to explore innovative therapeutic approaches capable of facilitating the reconstitution of the TBI-induced injury of the peripheral blood

cell populations following irradiation exposure. In response to these limitations and unmet needs, we have introduced a novel universal hematopoietic chimeric cell line, as a bridging rescue therapy for ARS.

The protocol for the creation of chimeric cells through PEG-mediated fusion has been developed and tested in our Laboratory over the past decade and applied for the creation of DRCC lines of different cell lineages (Cwykiel and Siemionow 2014; Siemionow et al. 2015, 2018a, b). We have tested DRCC efficacy in multiple studies on different animal models and demonstrated that the presence of multilineage chimerism prevents transplant rejection and extends allografts survival (Cwykiel et al. 2011, 2021a; Cwykiel and Siemionow 2015). These efforts have consistently confirmed the immunomodulatory and pro-tolerogenic properties of DRCC (Cwykiel and Siemionow 2015; Cwykiel et al. 2021a, b).

Encouraged by these promising results, our objective was to evaluate the DRCC effect on the animals' survival rate, the recovery of peripheral blood cell populations as well as the incidence of GvHD following TBI. In this study, we established an experimental rat model of TBI to assess, for the first time, the impact of DRCC on peripheral blood cell populations recovery, when compared to conventional ARS treatment involving alloBMT and the frequency of GvHD occurrence. A 7 Gy TBI nonlethal dose was employed, an irradiation level verified to induce ARS signs. The feasibility of the cell fusion procedure and the creation of DRCC were evaluated by FC and CM. The DRCC transplantation was performed using our well-established protocol of intraosseous cell injection (Siemionow et al. 2005a, b; Klimczak et al. 2007). The determination of the alloBMT and DRCC dose was based on our previous reports (Klimczak et al. 2007; Hivelin et al. 2016).

The survival assessment confirmed that the 7 Gy irradiation dose is nonlethal, as evidenced by the 100% survival rate observed in the control group injected with saline. In this study, transplantation of the alloBMT after TBI resulted in 60% mortality rate, in contrast to the 100% survival found in the animals treated with DRCC and the combined alloBMT + DRCC. These findings correlated with the least favorable clinical outcomes of animal's behavior, posture, fur coverage, and worst results of the complete blood counts observed following alloBMT injection when compared to other therapy groups. These outcomes confirm the superior efficacy of DRCC over the alloBMT therapy. More precisely, DRCC therapy reduced the harmful effect of alloBMT. Interestingly, administration of the combined alloBMT + DRCC resulted in 100% survival and better clinical outcomes measures confirming tolerogenic role of DRCC, when compared with the fully allogeneic response leading to high mortality after administration of alloBMT alone.

To investigate the impact of DRCC therapy following TBI, a 90-day body weight analysis was conducted. Weight changes were expressed as percentages of the initial weight to comprehensively evaluate the impact of different cellular therapies over the observation period. It should be noted that there were differences in the initial body mass among the experimental groups. The body weight analysis revealed a consistent and physiologically normal weight gain in all surviving animals. These findings substantiate the beneficial impact of the administered therapies on weight gain, which is crucial considering that TBI exposure often leads to weight loss, potentially culminating in fatality (Koch et al. 2016).

Following 7 Gy TBI, we observed a similar pattern of the acute response to irradiation injury in all therapy groups, which revealed a significant drop in all populations of WBC, RBC, and PLT starting on day 5 and lasting up to 20 days post-irradiation. From day 20 onward, there was a visible and significant rebound and recovery of all peripheral blood cell populations, which gradually returned to normal pre-TBI values starting around day 40 for DRCC therapy and around day 60 for other therapy groups. Finally, at day 90 post-TBI, all peripheral blood cell populations returned to pre-TBI levels. Daily assessments post-TBI revealed the following changes: between days 5 and 20, a significant leukopenia, characterized primarily by lymphocytopenia and monocytopenia, was observed. Subsequently, a robust peripheral blood cell populations recovery was demonstrated from day 20, maintained throughout the entire observation period, and reaching close to normal values between 30 days and 90 days in the DRCC and combined alloBMT + DRCC groups. Based on the presented outcomes, the DRCC therapy clearly facilitates early peripheral blood cell populations recovery post-TBI in contrast to the delayed response observed following alloBMT delivery. The observed beneficial effect of DRCC on the enhancement of the WBC, RBC, and PLT counts recovery can be attributed to the tolerogenic properties inherent to the chimeric cells, characterized by the hematopoietic (CD45), progenitor (CD90), and B cell (CD45A) surface markers (Cwykiel et al. 2021a, b). These unique DRCC characteristics underscore the potential for development of the multilineage chimerism after DRCC transplantation when compared to BMT, as confirmed in our previous studies (Cwykiel et al. 2021b). Additionally, the capacity of DRCC to secrete interleukin-10 and transforming growth factor beta further support their tolerogenic and immunomodulatory characteristics (Cwykiel et al. 2021a). Conversely, the allogeneic properties associated with BMT contributed to the delayed and reduced level of peripheral blood cell populations recovery compared to other tested therapies. However, the simultaneous administration of DRCC and alloBMT revealed better response to TBI-induced injury

in recovery of WBC confirmed by significantly higher monocytes counts, compared to the administration of the alloBMT alone, further confirming immunomodulatory effect of DRCC therapy. These findings can be attributed to the presence of the myeloid cell surface markers (CD11b/c, OX-82) on the DRCC, as we have previously reported (Cwykiel et al. 2011, 2021a, b). There were no significant changes in the levels of neutrophils, eosinophils, or basophils recorded in any of the therapy groups during the entire observation period. The results of our study align with the existing literature data, confirming that hematopoietic syndrome is among the earliest indications of ARS (Weisdorf et al. 2006). In ARS victims, blood counts demonstrated a significant decrease based on the received irradiation dose. For relatively low irradiation doses (2–4 Gy), endogenous recovery of autologous hematopoiesis would be expected. In contrast, individuals subjected to higher irradiation doses (6–10 Gy) would require allogeneic or, if available, cryopreserved autologous hematopoietic cell support (Baranov et al. 1989; Weisdorf et al. 2006; López and Martín 2011). The early occurrence of hematopoietic syndrome after TBI is attributed to the heightened sensitivity of blood cells to irradiation injury (Baranov et al. 1989; Weisdorf et al. 2006) with the lymphocytes, representing the most sensitive to irradiation blood cell line and exhibiting the initial symptoms of lymphopenia typically within 6–24 h after radiation exposure (Macià I Garau et al. 2011; Ossetrova et al. 2016; Jackson et al. 2021; Hollingsworth et al. 2023). In our study, a significant drop in the complete blood count including lymphopenia was observed up to 5 days following 7 Gy TBI followed by steady recovery, which correlated with transplantation of cellular therapies. Moreover, transplantation of DRCC following TBI contributed to more rapid recovery of the peripheral blood cell populations compared to the delayed response after alloBMT therapy. These encouraging results further confirmed tolerogenic and immunomodulatory effects of chimeric cells, thus establishing DRCC as a highly efficacious therapeutic measure, with potential clinical applications particularly in scenarios involving a large-scale radiation incident.

The review of literature related to TBI scientific data indicates that mature RBCs and PLTs, due to their lack of a nucleus, are relatively more resistant to irradiation (Macià I Garau et al. 2011; Cwykiel and Kwiecień 2015). In our study, assessment of RBC behavior after TBI confirmed this relative resistance, revealed by a mild anemia observed between 10 days and 20 days, followed by stabilization of the RBC values throughout the remaining 90-day observation period. Similarly, the initial thrombocytopenia observed between 5 days and 10 days post-TBI, was followed by the return to normal PLT values over the remaining observation period. Furthermore, throughout almost every stage of the follow-up, the PLT counts were consistently higher in the DRCC group

resembling the normal values from day 20 onward compared to the alloBMT group. This phenomenon may be elucidated by the intrinsic properties of DRCC to differentiate into progenitor and myeloid cells, as verified by our previous studies (Cwykiel et al. 2021a, b).

Moreover, this study confirmed that the transplantation of DRCC therapy following TBI was not linked with the development of GvHD based on both the clinical parameters and histopathological evaluation. The application of DRCC and combined alloBMT + DRCC therapies following TBI revealed nearly normal animal cage activity, body posture, and fur coverage, with the overall clinical assessments revealing the close to normal values recorded following administration of the DRCC therapy compared to other tested therapies. The acquired data revealed that, concomitant with clinical symptoms, notable histopathological changes indicative of GvHD were evident after administration of alloBMT, as opposed to the DRCC and combined alloBMT + DRCC therapies. The most pronounced changes were identified in the small intestine samples across all therapy groups, aligning with existing literature data that underscore the substantial contribution of gastrointestinal cell destruction to GvHD mortality (Schroeder and DiPersio 2011; Ghimire et al. 2017; Srinagesh et al. 2019). Histopathological changes observed in renal tissue samples exhibited a lower degree of intensity compared to the changes observed in small intestine samples. This discrepancy may be rationalized by the observation that histopathological symptoms in the kidneys are commonly discernible only in the chronic form of GvHD (Shulman et al. 2015; Srinagesh et al. 2019). Therefore, the 90-day observation period implemented in our study could account for the absence of advanced renal signs of GvHD.

There are several limitations of this study that need to be addressed and include the use of a specific rat strain and the inclusion of only male animals, which may limit the generalizability of these findings. Nevertheless, it lays the groundwork for future exploration of the mechanisms underlying DRCC action, with a focus on their involvement in immunoregulatory processes to promote the peripheral blood cell populations recovery applied after TBI without the risk of GvHD. These findings hold the potential for therapeutic applications of DRCC in the clinical scenario of ARS.

However, notwithstanding these limitations, our study signifies, for the first time, that DRCC can be applied as a rescue therapy in ARS. This investigation affirms that the proposed universal hematopoietic chimeric cell rescue therapy effectively mitigated both the acute and long-term toxic effects associated with exposure to nonlethal doses of ionizing irradiation. Additionally, administration of DRCC therapy after TBI extended recipients' survival when compared with the standard alloBMT.

Furthermore, the risk of GvHD, a severe and limiting complication of BM or stem cell transplantation, was markedly reduced in animals treated with DRCC. Therefore, our study emphasizes the role of DRCC therapy in facilitating faster and more effective cell engraftment and peripheral blood cell populations recovery following TBI. This ultimately would lead to improved outcomes in individuals exposed to TBI as DRCC could serve as the bridge therapy until an HLA-compatible donor would become available. Additionally, the potential for cryopreservation and the low immunogenicity of DRCC (Cwykiel and Kwiecień 2015) confirm the plausible clinical application of DRCC therapy. This entails DRCC manufacturing, cryopreservation, and banking at times of peace with the intent for off-the shelf availability and administration during periods of high demand such as nuclear disasters. Consequently, DRCC therapy holds significant promise for cost reduction and the elimination of side effects associated with the currently used alloBMT and immunomodulatory protocols.

Therefore, DRCC therapy represents a novel and unique approach for the mitigation of TBI-induced complications and amelioration of ARS signs.

Acknowledgments

The authors thank Joanna Cwykiel, PhD for technical support and data acquisition as well as the staff members of the Radiation Safety Department of the University of Illinois at Chicago for the technical support and the staff members of the Biologic Resources Laboratory at University of Illinois at Chicago for technical assistance with processing blood sample analysis. The authors thank Andres Martin Acosta, MD from the Department of Pathology at the University of Illinois at Chicago for conducting the histological assessment of the tissue samples. We thank staff members of Flow Cytometry Core at University of Illinois at Chicago for technical assistance with acquisition of flow cytometry data. The authors would like to thank the BioRender software (Science Suite Inc., Toronto, Canada, RRID: SCR_018361) service, which was utilized to create Figures 1 and 2a.

Funding

This work was supported by the Defense Advanced Research Projects Agency (DARPA) DARPA-BAA-14-38 effort under Award No. W911NF-14-1-0323 and the U.S. Army Contracting Command – Aberdeen Proving Ground (ACC-APG), 4300 Miami Boulevard Durham, NC 27703. Opinions, interpretations, conclusions, and recommendations are those of the authors and are not necessarily endorsed by the Department of Defense.

Ethics Approval

This study was approved by the Institutional Animal Care and Use Committee (IACUC) of University of Illinois at Chicago, which is accredited by the American Association for the Accreditation of Laboratory Animal Care (AAALAC).

Authors' Contributions

MS: conception and design of study, data analysis and interpretation, manuscript writing, final manuscript approval. MC: collection of data, data analysis and interpretation, manuscript writing. KS: collection and assembly of data, data analysis and interpretation, manuscript writing. LC: data analysis and interpretation, manuscript writing. KK: critical review and final manuscript approval. All authors read and approved the final manuscript to be published.

References

- Baranov A, Gale RP, Guskova A et al (1989) Bone marrow transplantation after the Chernobyl nuclear accident. *N Engl J Med* 321:205–212. <https://doi.org/10.1056/NEJM198907273210401>
- Basic-Jukić N, Labar B (2003) [Immunosuppressive drugs in the prevention and treatment of GVHD after allogeneic bone marrow transplantation] (in Croatian). *Acta Med Croatica* 57:131–139.
- Billingham RE (1966) The biology of graft-versus-host reactions. *Harvey Lect* 62:21–78.
- Coeytaux K, Bey E, Christensen D et al (2015) Reported radiation overexposure accidents worldwide, 1980-2013: A systematic review. *PLoS One* 10:e0118709. <https://doi.org/10.1371/journal.pone.0118709>
- Cwykiel J, Jundzill A, Klimczak A et al (2021a) Donor recipient chimeric cells induce chimerism and extend survival of vascularized composite allografts. *Arch Immunol Ther Exp* 69:13. <https://doi.org/10.1007/s00005-021-00614-9>
- Cwykiel J, Klimczak A, Jundzill A et al (2011) Therapeutic potential of ex-vivo fused chimeric cells in prolonging vascularized skin allograft survival. *Plast Reconstr Surg* 127:26. <https://doi.org/10.1097/01.prs.0000396723.40767.22>
- Cwykiel J, Kwiecień GJ (2015) Cellular therapies in post-radiation syndrome. In: Siemionow M (ed) *Plastic and reconstructive surgery: Experimental models and research designs*. Springer, London, Heidelberg, New York, pp 629–636.
- Cwykiel J, Madajka-Niemeyer M, Siemionow M (2021b) Development of donor recipient chimeric cells of bone marrow origin as a novel approach for tolerance induction in transplantation. *Stem Cell Investig* 8:8. <https://doi.org/10.21037/sci-2020-044>
- Cwykiel J, Siemionow M (2014) Cellular therapy models: Ex vivo chimera model by cell fusion. *Plast Reconstr Surg* 29:593–603. https://doi.org/10.1007/978-1-4471-6335-0_72
- Cwykiel J, Siemionow M (2015) In vivo chimera model: Creation of primary and secondary chimera. In: Siemionow M (ed) *Plastic and reconstructive surgery: Experimental models and research designs*. Springer, London, Heidelberg, New York, pp 581–591.
- Ghimire S, Weber D, Mavin E et al (2017) Pathophysiology of GvHD and other HSCT-related major complications. *Front Immunol* 8:79. <https://doi.org/10.3389/fimmu.2017.00079>
- Gourmelon P, Benderitter M, Bertho JM et al (2010) European consensus on the medical management of acute radiation syndrome and analysis of the radiation accidents in Belgium and Senegal. *Health Phys* 98:825–832. <https://doi.org/10.1097/HP.0b013e3181ce64d4>
- Hagby M, Goldberg A, Becker S et al (2009) Health implications of radiological terrorism: Perspectives from Israel. *J Emerg Trauma Shock* 2:117–123. <https://doi.org/10.4103/0974-2700.50747>
- Heslet L, Bay C, Nepper-Christensen S (2012) Acute radiation syndrome (ARS) – Treatment of the reduced host defense. *Int J Gen Med* 5:105–115. <https://doi.org/10.2147/IJGM.S22177>
- Hirama T, Tanosaki S, Kandatsu S et al (2003) Initial medical management of patients severely irradiated in the Tokai-mura accident. *Br J Radiol* 76:246–253. <https://doi.org/10.1259/bjr/82373369>
- Hivelin M, Klimczak A, Cwykiel J et al (2016) Immunomodulatory effects of different cellular therapies of bone marrow origin on chimerism induction and maintenance across MHC barriers in a face allotransplantation model. *Arch Immunol Ther Exp* 64: 299–310. <https://doi.org/10.1007/s00005-015-0380-8>
- Hollingsworth BA, Aldrich JT, Case CM Jr et al (2023) Immune dysfunction from radiation exposure. *Radiat Res* 200:396–416. <https://doi.org/10.1667/RADE-22-00004.1>

Competing Interests

The authors have no relevant financial or nonfinancial interests to disclose.

Data Availability

All data generated and/or analyzed during the current study are included in this published article and are available for presentation from the corresponding author on reasonable request.

Consent to Participate

Not applicable.

Consent to Publish

Not applicable.

- Jackson IL, Gurung G, Ayompe E et al (2021) Characterization of the hemorrhagic syndrome in the New Zealand white rabbit model following total body irradiation. *Int J Radiat Biol* 97:S32–S44. <https://doi.org/10.1080/09553002.2020.1820601>
- Klimczak A, Unal S, Jankowska A et al (2007) Donor-origin cell engraftment after intraosseous or intravenous bone marrow transplantation in a rat model. *Bone Marrow Transplant* 40: 373–380. <https://doi.org/10.1038/sj.bmt.1705743>
- Koch A, Gulani J, King G et al (2016) Establishment of early endpoints in mouse total-body irradiation model. *PLoS One* 11:e0161079. <https://doi.org/10.1371/journal.pone.0161079>
- Lim M, Wang W, Liang L et al (2018) Intravenous injection of allogeneic umbilical cord-derived multipotent mesenchymal stromal cells reduces the infarct area and ameliorates cardiac function in a porcine model of acute myocardial infarction. *Stem Cell Res Ther* 9:129. <https://doi.org/10.1186/s13287-018-0888-z>
- López M, Martín M (2011) Medical management of the acute radiation syndrome. *Rep Pract Oncol Radiother* 16:138–146. <https://doi.org/10.1016/j.rpor.2011.05.001>
- Macià I, Garau M, Lucas Calduch A, López EC (2011) Radiobiology of the acute radiation syndrome. *Rep Pract Oncol Radiother* 16:123–130. <https://doi.org/10.1016/j.rpor.2011.06.001>
- Mettler FA Jr., Gus'kova AK, Gusev I (2007) Health effects in those with acute radiation sickness from the Chernobyl accident. *Health Phys* 93:462–469. <https://doi.org/10.1097/01.HP.0000278843.27969.74>
- Moris D, Cendales LC (2021) Sensitization and desensitization in vascularized composite allotransplantation. *Front Immunol* 12:682180. <https://doi.org/10.3389/fimmu.2021.682180>
- Ossetrova NI, Ney PH, Condliffe DP et al (2016) Acute radiation syndrome severity score system in mouse total-body irradiation model. *Health Phys* 111:134–144. <https://doi.org/10.1097/HP.0000000000000499>
- Ostheim P, Don Mallawaratchy A, Müller T et al (2021) Acute radiation syndrome-related gene expression in irradiated peripheral blood cell populations. *Int J Radiat Biol* 97:474–484. <https://doi.org/10.1080/09553002.2021.1876953>
- Schroeder MA, DiPersio JF (2011) Mouse models of graft-versus-host disease: Advances and limitations. *Dis Model Mech* 4: 318–333. <https://doi.org/10.1242/dmm.006668>
- Shulman HM, Cardona DM, Greenson JK et al (2015) NIH Consensus development project on criteria for clinical trials in chronic graft-versus-host disease: II. The 2014 Pathology Working Group Report. *Biol Blood Marrow Transplant* 21:589–603. <https://doi.org/10.1016/j.bbmt.2014.12.031>
- Siemionow M, Cwykiel J, Chambily L, Gacek S, Brodowska S. Novel Human Umbilical Di-Chimeric (HUDC) cell therapy for transplantation without life-long immunosuppression. *Stem Cell Investig*. 2023 Aug 14;10:16; <https://doi.org/10.21037/sci-2023-02>
- Siemionow M, Cwykiel J, Marchese E et al (2018b) A novel human myoblast chimeric cells therapy for restoration of muscle function. *Transplantation* 102:S355. <https://doi.org/10.1097/01.tp.0000543097.21030.13>
- Siemionow M, Cwykiel J, Madajka M (2015) Bone marrow-derived ex vivo created hematopoietic chimeric cells to support engraftment and maintain long-term graft survival in reconstructive transplantation. In: Brandacher G (ed) *The science of reconstructive transplantation*. Stem Cell Biology and Regenerative Medicine. Humana Press, New York, NY, pp 227–254. https://doi.org/10.1007/978-1-4939-2071-6_16
- Siemionow M, Cwykiel J, Heydemann A et al (2018a) Creation of dystrophin expressing chimeric cells of myoblast origin as a novel stem cell based therapy for Duchenne muscular dystrophy. *Stem Cell Rev Rep* 14:189–199. <https://doi.org/10.1007/s12015-017-9792-7>
- Siemionow MZ, Klimczak A, Unal S (2005a) Different routes of donor-derived hematopoietic stem cell transplantation for donor-specific chimerism induction across MHC barrier. *Transplant Proc* 37:62–64. <https://doi.org/10.1016/j.transproceed.2004.12.216>
- Siemionow M, Zielinski M, Ozmen S et al (2005b) Intraosseous transplantation of donor-derived hematopoietic stem and progenitor cells induces donor-specific chimerism and extends composite tissue allograft survival. *Transplant Proc* 37:2303–2308. <https://doi.org/10.1016/j.transproceed.2005.03.127>
- Srinagesh HK, Levine JE, Ferrara JLM (2019) Biomarkers in acute graft-versus-host disease: New insights. *Ther Adv Hematol* 10:2040620719891358. <https://doi.org/10.1177/2040620719891358>
- Weisdorf D, Chao N, Waselenko JK et al (2006) Acute radiation injury: Contingency planning for triage, supportive care, and transplantation. *Biol Blood Marrow Transplant* 12:672–682. <https://doi.org/10.1016/j.bbmt.2006.02.006>